

INVESTIGATIONS OF INTERLAMINAR FRACTURE TOUGHNESS OF LAMINATED POLYMERIC COMPOSITES¹

A. Korjakin,* R. Rikards,*
F.-G. Buchholz,** H. A. Richard,**
A. K. Bledzki,*** and H. Wang**

The behavior of interlaminar fracture of fiber-reinforced laminated polymeric composites has been investigated in modes I, II, and different mixed mode I/II ratios. The experimental investigations were carried out by using conventional beam specimens and the compound version of the CTS (compact tension shear) specimen. In this study, a compound version of the CTS specimen is used for the first time to determine the interlaminar fracture toughness of composites. In order to verify the results obtained by the CTS tests, conventional beam tests were also carried out. In the beam tests, specimens of double cantilever beam (DCB) and end notched flexure (ENF) were used to obtain the critical rates of the energy release for failure modes I and II. The CTS specimen is used to obtain different mixed mode ratios, from pure mode I to pure mode II, by varying the loading conditions. The highest mixed mode ratio obtained in the experiment was $G_I/G_{II} = 60$. The data obtained from these tests were analyzed by the finite element method. The separated critical rates G_I and G_{II} of the energy release were calculated by using the modified virtual crack closure integral (MVCCI) method. The experimental investigations were performed on a unidirectional glass/epoxy composite. The results obtained by the beam and CTS tests were compared. It was found that the interlaminar fracture toughness G_{IC}^{init} of mode I at crack initiation and the corresponding value G_{IIC}^{init} of mode II obtained by the conventional beam and the CTS tests were in rather good agreement. The experimental results of interlaminar fracture of mixed mode were used to obtain the parameters required for the failure criterion. The two different failure criteria were compared. The best correlation with the experimental data was obtained by using the failure criterion proposed by Wu in 1967 containing linear and quadratic terms of the rates of the energy release.

1. Introduction

Interlaminar fracture behavior of laminated polymeric composites has widely been investigated. A brief review of these investigations was given in [1]. The main problem in predicting the failure of laminated composite materials is the evaluation of interlaminar fracture toughness under conditions of mixed mode loading. Various approaches have been used to develop test specimens for combined or mixed mode loading;

¹ Presented at the 10th International Conference on the Mechanics of Composite Materials (Riga, April 20-23, 1998).

*Institute of Computer Analysis of Structures, Riga Technical University, LV-1658 Riga, Latvia; **Institute of Applied Mechanics, University of Paderborn, D-33098 Paderborn, Germany; ***Institute of Material Science, University of Kassel, D-34109 Kassel, Germany. Translated from Mekhanika Kompozitnykh Materialov, Vol. 34, No. 3, pp. 307-322, May-June, 1998. Original article submitted January 2, 1998.

however, extensive research has mainly been focused on mode I and II interlaminar fracture behavior of composite materials. Double cantilever beam (DCB) and end notched flexure (ENF) specimens have been employed for mode I and II tests, respectively. Also in the mixed mode tests, mainly beam type specimens were used in order to obtain the critical rates of the energy release of mixed mode I/II.

The tests of mixed mode I/II are characterized by the G_I/G_{II} ratio of the rates of energy release that are driving the crack. Various G_I/G_{II} ratios of mixed mode can be obtained by using different specimens. The mixed mode flexure (MMF) test is mode I dominating with a ratio of $G_I/G_{II} = 1.33$ obtained from the linear beam analysis [2]. This ratio is valid when the upper and lower parts of the specimen are of equal thickness. However, as shown in [1, 3] for the MMF specimen, the mixed mode ratio obtained by the finite element solution is dependent on the crack length and varies from 1.4 to 1.5. By varying the thickness ratio of the lower and upper parts, different mixed mode I/II ratios can be obtained [3]. In the case where the so-called end-loaded split (ELS) specimen is loaded by the upper arm also the conditions of mixed mode loading at the crack tip are achieved. For a symmetrical geometry, the mixed mode I/II ratio obtained from the linear beam analysis here also is $G_I/G_{II} = 1.33$ [5].

Very similar to the MMF specimen is the so-called single leg bending (SLB) specimen [3] for which only the supports are of different height. With this specimen different mixed mode I/II ratios can also be achieved, while mode I remains dominant. By the crack lap shear (CLS) test also various G_I/G_{II} ratios can be achieved by varying the stepped thickness ratio; however, in this case mode II is dominant [2]. The crack growth for the CLS test is semistable and it is possible to record several data points with the crack growth. However, these test measurements suffer from large scatter with increasing of the crack length [2]. The mixed mode loading can be generated also by using an edge delamination tension (EDT) specimen [6]. Furthermore, different mixed mode I/II ratios from 44 to 56% of the total fracture energy for mode II can be achieved by the specimen of mixed mode bending employed in [7].

For all the specimens of mixed mode discussed above, there are limited possibilities to achieve a broad range of the ratios of mixed mode. However, this can be achieved by loading the ENF specimen by a special loading lever. This is the so-called test of mixed mode bending (MMB) proposed in [8]. The MMB test just combines the tests of mode I DCB and mode II ENF and by different loading positions various ratios of the mixed mode are achieved. In [8], the experiments were carried out with G_I/G_{II} ratios from 0.25 to 4, whereas in [9] they varied even from 0.002 to 35. Now the MMB specimen is widely used in order to determine the critical rates of the energy release of mixed mode for different composites [8-10]. Still the disadvantage of all specimens of beam type is that for pure mode I as well as for different ratios of mixed mode I/II different specimens of the beam type have to be used. For example, to establish the fracture criterion for delamination, four different beam specimens (DCB, ENF, CLS and modified ENF) were used in [11]. In order to obtain reliable results for the interlaminar fracture toughness under different conditions of combined or mixed mode loading starting from pure mode I to II, it is desirable that only one type of the specimens be required. Since this was almost impossible to achieve by using beam type specimens, other types of test specimens have also been developed. One type is the so-called Arcan specimen, which was first employed for combined loading of composites [12], then for fracture tests of isotropic materials [13], and also for tests of mixed mode fracture of composites [14, 15]. Another type of specimens for studying the properties of interlaminar fracture of laminated composites is the Iosipescu specimen [16].

The most recent development is the compound version of the compact tension-shear (CTS) specimen which covers all conditions of the in-plane mixed mode loading from pure mode I through any ratio of mixed mode I/II up to pure mode II. The CTS specimen was proposed in [17, 18] for fracture tests of isotropic materials under these general loading conditions. In this study, the compound version of the CTS specimen is used for studies of mode I, mixed mode I/II, and mode II properties of interlaminar fracture toughness of the glass/epoxy composite. For loading of pure mode I and II, the results obtained by the CTS tests have been compared with those obtained by the beam tests. A detailed description of the beam tests was given in [1].

2. Experimental

2.1. Material. For the production of the composite material considered in this investigation, glass fibers from Owens Corning Ltd. and a ductile epoxy matrix with an ultimate strain of 7.7% at failure in tension (Araldite epoxy resin of Ciba Geigy Ltd.) were used. The glass/epoxy composite investigated in this study is similar to the material investigated previously [1], where a brittle epoxy matrix with an ultimate strain of 3.3% at failure in tension was used. A more ductile matrix is used in order to reduce the influence of the imperfections since in the CTS test the width of the composite specimen is only 10 mm. For the beam tests, the specimen width is 25 mm, i.e., the same as previously [1]. In [1], glass fibers sized with polyethylene or silane coupling agents were tested, whereas in this investigation industrial fibers with standard surface treatment are used.

Plates of unidirectionally (UD) reinforced glass fiber were produced through winding technology and in the production of the composite 68-69 TEX (g/1000 m) roving was used. The plates contained a starter crack introduced by a Teflon film (thickness 40 μm) placed between the central plies. The total number of the plies was 12 in order to obtain a plate of 3 mm thickness. The laminates were produced according to the standard cure cycle recommended by Ciba Geigy Ltd. In order to improve the quality of the plates and to reduce the content of voids, the plates were placed in vacuum before curing. The specimens (composite strips of 10 mm width) were cut out with a diamond wheel and kept at room temperature until testing (23°C and 50% of relative humidity). All the tests were performed under the same conditions. The content of the fiber volume of the specimens was 50%. In the calculations, the composite strip is considered to be a homogeneous transverse isotropic material.

2.2. Compound Version of the CTS Specimen. The CTS (compact tension-shear) specimen (see Fig. 1) proposed in 1983 by Richard [17, 18] for the investigations of the mixed mode fracture of isotropic materials can also be used with some modifications for laminated composites. This compound version of the CTS specimen (see Fig. 2) is used in this study in order to investigate the interlaminar fracture toughness of laminated composites. A strip of the edge cracked composite is glued into glassmat/epoxy blocks. These blocks are again glued into aluminum end blocks in order to carry the applied loads. The intermediate glassmat/epoxy blocks must be of about the same modulus of elasticity as the transverse modulus of the composite strip in order to reduce the influence of the composite strip/block interface on the stress field at the crack tip.

The forces F_i ($i = 1, 2, \dots, 6$) acting on the holes of the CTS specimen (see Fig. 2) can be calculated by the relations [17]

$$\begin{aligned} F_3 &= F_4 = P \left(\frac{1}{2} \cos \alpha + \frac{c}{b} \sin \alpha \right), \\ F_2 &= F_5 = P \sin \alpha, \\ F_1 &= F_6 = P \left(\frac{1}{2} \cos \alpha - \frac{c}{b} \sin \alpha \right), \end{aligned} \quad (1)$$

where α is the loading angle (see Fig. 1). In the finite element analysis, these forces are applied to the corresponding nodes of the finite element mesh.

The advantage of the compound version of the CTS specimen is that with the same test specimen all combinations of the ratios of plane mixed mode from pure mode I to II can be achieved. In this study, the experiments were carried out for pure mode I ($\alpha = 0^\circ$), pure mode II ($\alpha = 90^\circ$), and the mixed mode with $\alpha = 75, 78, 81, 84, \text{ and } 87^\circ$, i.e., for the ratios of mixed mode where mode II is dominant.

For the experiments, the testing machine Zwick 1446 was used. The specimens were tested by loading at a constant displacement rate of 0.5 mm/min. The critical load P_c and the corresponding displacement in the direction of the load P were measured. In all cases, an unstable growth of cracks was observed. By using

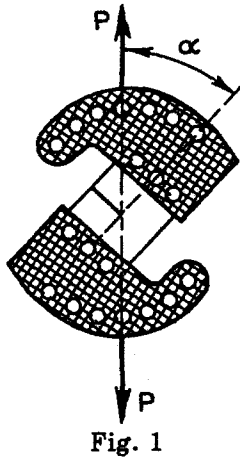


Fig. 1

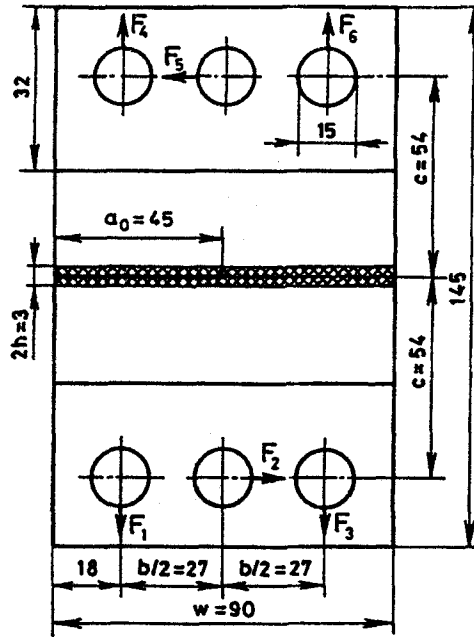


Fig. 2

Fig. 1. Loading scheme of the CTS specimen.

Fig. 2. Geometry of the compound version of the CTS specimen (width of specimen $t = 10$ mm, dimensions of specimen in mm).

the compound version of the CTS specimen, altogether 28 samples of the laminated composite were tested for the various ratios of the mixed mode.

3. Finite Element Analysis

A finite element model of the specimen (see Fig. 3) consists of 2681 quadrilateral plane strain elements with 4 nodal points (linear approximation of the displacements within the element) and there are altogether 7310 degrees of freedom (DOF). The loads to the specimen are applied according to Fig. 2 and are calculated by the expressions (1). The finite element analysis was performed with the ABAQUS program [19].

For the calculation of the G_I and G_{II} rates of the energy release, the modified virtual crack closure integral (MVCCI) method is used. Then the separated rates of the strain energy release are obtained by only one calculation (the MVCCI or 1C method) for the actual length a of the crack as proposed in [20] (see Fig. 4)

$$G_I^{1C}(a) = \frac{1}{t} \frac{1}{\Delta a} \frac{1}{2} [F_y^i(a) \Delta u_y^{i-1}(a)], \quad G_{II}^{1C}(a) = \frac{1}{t} \frac{1}{\Delta a} \frac{1}{2} [F_x^i(a) \Delta u_x^{i-1}(a)], \quad (2)$$

where $F_x^i(a)$ and $F_y^i(a)$ are the forces of the nodal point at the crack tip node i in the x and y directions, respectively, while $\Delta u_x^{i-1}(a)$ and $\Delta u_y^{i-1}(a)$ are the relative displacements of the nodal point of the opposite faces of the crack at node $i-1$ in the x and y directions, respectively. Therefore, $\Delta u_x^{i-1}(a)$ is the displacement of the crack sliding, while $\Delta u_y^{i-1}(a)$ is the displacement of the crack opening at a distance Δa behind the crack tip and

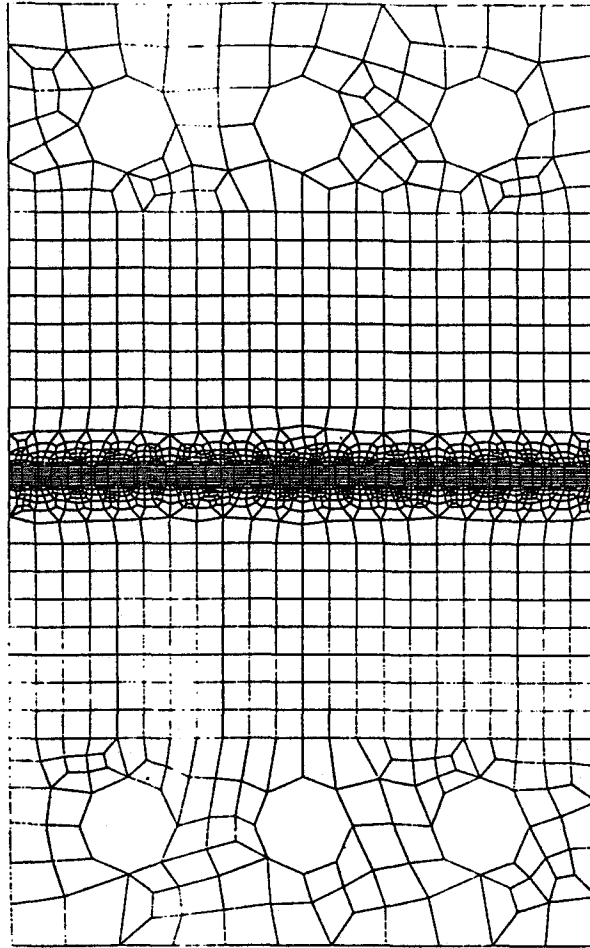


Fig. 3. Finite element mesh for the CTS specimen.

$t = 10$ mm is the width of the specimen. In the finite element model, the crack increment $\Delta a = 0.5$ mm was used.

The rates of the energy release were calculated by using the elastic properties of different parts of the compound CTS specimen. For the glassmat/epoxy blocks (transverse isotropic material with reinforcement in plane 1-2), the properties are as follows:

$$E_1 = E_2 = 5.7 \text{ GPa}, \quad \nu_{12} = 0.35, \quad G_{12} = E_1/2(1 + \nu_{12}).$$

For the aluminum blocks (isotropic material), the Young's modulus and Poisson's ratio are given by

$$E = 70 \text{ GPa}, \quad \nu = 0.30.$$

For the composite strip (transverse isotropic material with the fibre direction 1), the elastic properties are as follows:

$$E_1 = 40.7 \text{ GPa}, \quad E_2 = 10.27 \text{ GPa}, \quad G_{12} = 4.2 \text{ GPa}, \quad \nu_{12} = 0.27, \quad \nu_{23} = 0.29.$$

By using these properties, the finite element solution for the compound CTS specimen with the initial crack $a = 45$ mm (see Fig. 2) was obtained. The rates of the energy release were calculated by the expressions (2). The calculated ratios of the mixed mode of the compound version of the CTS specimen are presented in Table 1. It should be noted that for testing isotropic materials an increment of $\Delta\alpha = 15^\circ$ for increasing the loading angle stepwise from $\alpha = 0^\circ$ (pure mode I) to $\alpha = 90^\circ$ (pure mode II) was reasonable and sufficient (see Fig. 1). However, for the investigations of the interlaminar fracture behavior of composites, it is of practical

TABLE 1. Ratios of the Mixed Mode of the Compound Version of the CTS Specimen under Different Loading Angles α

α	0°	15°	30°	45°	60°	75°	78°	81°	84°	87°	90°
G_{II}/G_I	0	0.001	0.045	0.136	0.416	2.0	3.17	5.80	13.0	59.9	∞

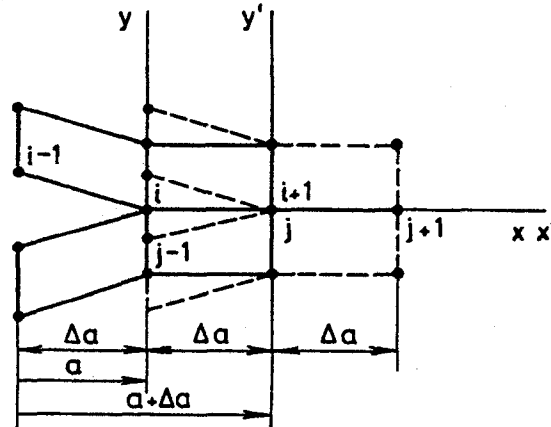


Fig. 4. Finite element mesh and nodal point numbering near the crack tip for the modified virtual crack closure integral (MVCCI) method.

interest to achieve experimentally higher ratios of mode II and I. Therefore, an additional loading device was designed and applied, by which $\Delta\alpha = 3^\circ$ was realized in the experiments for $75^\circ < \alpha < 90^\circ$. The highest ratio of mode II and I achieved in this investigation was about 60 (see Table 1). In Fig. 5, the values of the ratios of the mixed mode versus the loading angle are presented. It is seen that for loading angles close to 90° very high ratios of mode II and I can be achieved. On the other hand, for loading angles between 0 and 15° very high ratios of mode I and II can be achieved. Therefore, by using the compound version of the CTS specimen all the ratios of the mixed mode from pure mode I to II can be achieved and tested. It should be noted that the ratios of the mixed mode depend on the geometry and stiffness properties of the composite strip, the glassmat/epoxy, and the end blocks, but they are obtained from the finite element solution.

4. Results and Failure Criterion

The experimentally measured critical loads P_c were employed in order to calculate the separated critical rates G_{IC} and G_{IIC} of the energy release. It is of interest to compare the results obtained by the compound version of the CTS specimen with the results obtained by the beam tests. The same laminated composites were tested by using the double cantilever beam (DCB) specimen (four samples) and the end notched flexure (ENF) specimen (four samples). The critical rates G_{IC} of the energy release of mode I at the crack initiation obtained by the DCB test and the critical rates G_{IIC} of the energy release of mode II obtained by the ENF test were compared with the corresponding values obtained by the CTS test. The results are presented in Table 2.

The data reduction for the DCB and ENF tests were performed by using linear beam analysis since only the crack initiation values have been calculated [1, 4]. From the comparison of the results presented in Table 2, it can be concluded that the mean values obtained by the beam tests are in the 95% confidence limits of the results obtained by the CTS test. A good agreement of the mean values obtained by different test methods can also be observed for the critical rate G_{IIC} of the energy release of mode II. The differences for the mean values are only about 2.5%. In the case of mode I loading, the differences between the mean values are larger

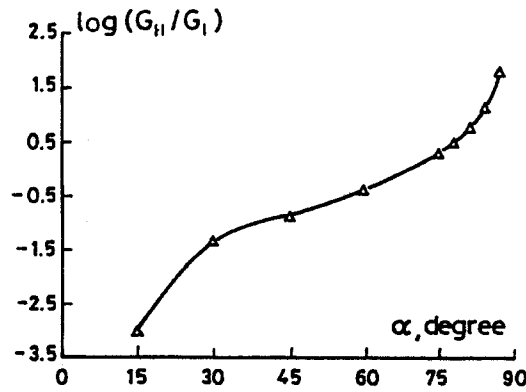


Fig. 5. G_{II}/G_I ratios of the energy release rates of the mixed mode (in the logarithmic scale) versus the loading angle α of the CTS specimen.

TABLE 2. Mean Values and 95% Confidence Limits of the Critical Rates of Energy Release Obtained by the CTS and Beam Tests

Fracture parameter	CTS	Beam	
		DCB	ENF
G_{IC} , kJ/m ²	0.227±0.0835	0.144±0.0219	—
G_{IIC} , kJ/m ²	1.66±0.496	—	1.62±0.218

because the mean value of G_{IC} obtained by the DCB test is by 36% lower than that obtained in the CTS test. However, the mean value obtained by the DCB test is also within the confidence limits of the result obtained by the CTS test. Therefore, in the case of pure mode I or II loading, there are no statistically significant differences between the results obtained by the beam and the CTS tests and both results can be used for the evaluation of the parameters for the fracture (failure) criterion.

In [21-26], a number of fracture criteria of mixed mode have been proposed in order to describe the interlaminar fracture of composites. These criteria are similar to those used for isotropic materials. The fracture criteria can be formulated for different parameters of the crack tip fracture as the stress intensity factor (SIF) or the energy release rate for which the critical fracture parameters (K_C or G_C) can be determined experimentally. Previously, the stress intensity factors were mainly used as fracture parameters, while for composites the energy release rates, which also are used in this study, seem to be more useful and common.

In [21], Wu proposed the following empirical relationship for the evaluation of fracture of mixed mode of balsa wood or glass fiber-reinforced plastic:

$$\frac{K_I}{K_{IC}} + \left(\frac{K_{II}}{K_{IIC}}\right)^2 = 1. \quad (3)$$

This criterion was also used in [22] for the evaluation of fracture of mixed mode of graphite/epoxy composites. In [22], the parameters K_{IC} and K_{IIC} for the criterion (3) were obtained by the method of least squares.

The fracture criterion of mixed mode can also be written in a more general form [23, 24]

$$\left(\frac{K_I}{K_{IC}}\right)^m + \left(\frac{K_{II}}{K_{IIC}}\right)^n = 1. \quad (4)$$

TABLE 3. Parameters of Criterion (5) Obtained by the Method of Least Squares

Criterion	G_{IC} , kJ/m ²	G_{IIC} , kJ/m ²	f
$m = 1; n = 2$	0.175	1.561	0.878
$m = 2; n = 2$	0.156	1.503	1.193

The quadratic form of this criterion was used in [14] to evaluate the interlaminar fracture behavior of the graphite/epoxy material under loading conditions of mixed mode. In (4), the rates of the energy release can be used instead of the stress intensity factors

$$\left(\frac{G_I}{G_{IC}}\right)^m + \left(\frac{G_{II}}{G_{IIC}}\right)^n = 1. \quad (5)$$

In [25], it was pointed out that for graphite/thermoplastic materials the best fitting criterion was found with the exponents $m = 1$ and $n = 3/2$ in Eq. (5). For the graphite/epoxy material presented in [25], a lower bound (i.e., most of the data lie outside the failure surface) was obtained with $m = 1$ and $n = 1$ in Eq. (5). However, the best fitting criterion for the graphite/epoxy material is of the exponential form [25]

$$G_I + G_{II} + e^{-(c_1 M + c_2)} - c_3 = 0 \quad (6)$$

with

$$M = \sqrt{1 + G_{II}/G_I \sqrt{E_1/E_2}},$$

where c_1 , c_2 , and c_3 are empirical parameters and E_1 , E_2 are Young's moduli of the composite.

In [26], it was proposed to use a nonconvex criterion for failure of the mixed mode of composites. It was shown that for PEEK-matrix/carbon-fiber composites the concave criterion [26] gives good agreement with the experimental data for the values of the crack propagation.

In this study, the approximation of the results obtained by the CTS test were carried out by using the criterion (5). Two variants of the criterion for the exponents $m = 1$, $n = 2$ or $m = 2$, $n = 2$ were analyzed. The approximations were performed using the method of least squares in the polar coordinates $G_I = \rho \cos \varphi$; $G_{II} = \rho \sin \varphi$, i.e., by minimizing the cost function $f(\mathbf{x})$

$$f(\mathbf{x}) = \sum_{i=1}^N [\rho(\mathbf{x}) - \rho_i]^2. \quad (7)$$

Here, $\rho(\mathbf{x})$ corresponds to the criterion (5) in the polar coordinates, while $\mathbf{x} = \{G_{IC}, G_{IIC}\}$ contains the parameters of optimization, ρ_i are the experimental values of the critical rates of energy release in the polar coordinates, and N is the total number of experimental points (in our case $N = 36$, i.e., 28 points were obtained by the CTS test and, in addition, 8 points were obtained by the beam tests). The results of the minimization of the cost function (7) are presented in Table 3, where f is the value of the function $f(\mathbf{x})$ at the point of optimum $\mathbf{x}^*(f = f(\mathbf{x}^*))$. The approximation is better for the lower value of the cost function. It is seen that a better approximation was obtained for the exponents $m = 1$ and $n = 2$ in the criterion (5). Both approximations used here are shown in Fig. 6.

Further on, a more detailed analysis is performed for $m = 1$ and $n = 2$ in the criterion (5). In Fig. 6, a rather big scatter of the experimental values of the interlaminar fracture toughness can be seen. It is of interest to calculate the confidence limits for the criterion. In Fig. 7 the 95% confidence limits are presented, and the mean values of the critical rates of energy release for various ratios of the mixed mode are shown. It can be observed that the mean values for all the ratios of the mixed mode are within the 95% confidence

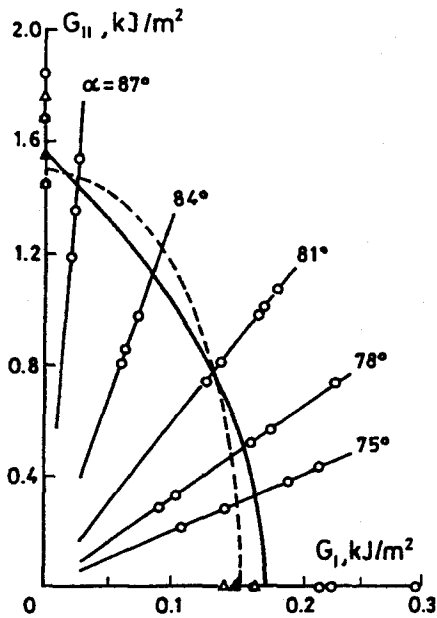


Fig. 6

Fig. 6. Approximation of the experimental data of the mixed mode for criterion (5) with $m = 1, n = 2$ and $m = 2, n = 2$. \circ — CTS, \triangle — beam.

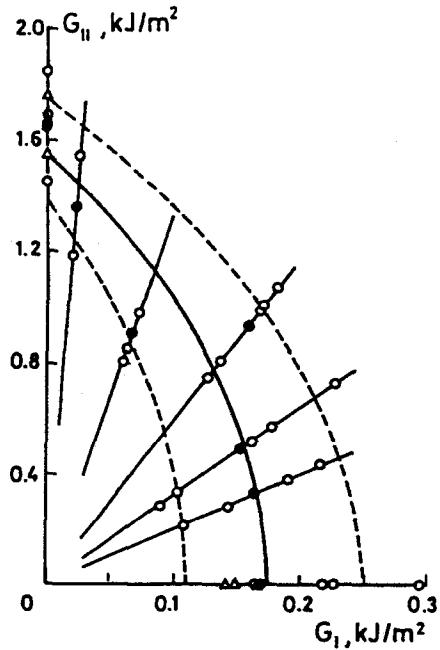


Fig. 7

Fig. 7. Criterion (5) with $m = 1, n = 2$ and 95% confidence limits. \circ — CTS, \triangle — beam, \bullet — mean.

limits. Therefore, the criterion (5) for the exponents $m = 1$ and $n = 2$ and the CTS tests for different ratios of mixed mode I/II give results that are within the 95% confidence limits.

By introducing a comparative rate G_V of the energy release, the fracture criterion (5) for the exponents $m = 1$ and $n = 2$ can be written in the form [27]

$$G_V = \frac{G_I}{2} + \frac{1}{2} \sqrt{G_I^2 + 4(\alpha_1 G_{II})^2} \leq G_{IC}. \quad (8)$$

Here, a new material constant α_1 is introduced,

$$\alpha_1 = G_{IC}/G_{IIC}, \quad (9)$$

which denotes the ratio of the fracture toughness of mode I and II. From Table 3, it is seen that for the composite investigated in this study $\alpha_1 = 0.112$. Then, the energy required to drive the crack of mode II is about nine times higher than that for the crack of mode I.

It is also of interest to compare the rates of energy release under different loading angles α of the CTS specimen for a constant value of the load $P = 1000$ N (see Fig. 1). In Fig. 8, the comparative energy G_V , the rate G_{II} of the energy release of mode II, and the rate $G_T = G_I + G_{II}$ of the total energy release are presented as functions of the loading angle α . The rate G_I of the energy release of mode I is practically equal to the comparative energy G_V from $\alpha = 0^\circ$ to $\alpha = 60^\circ$. Therefore, for a broad range of loading angles for the criterion

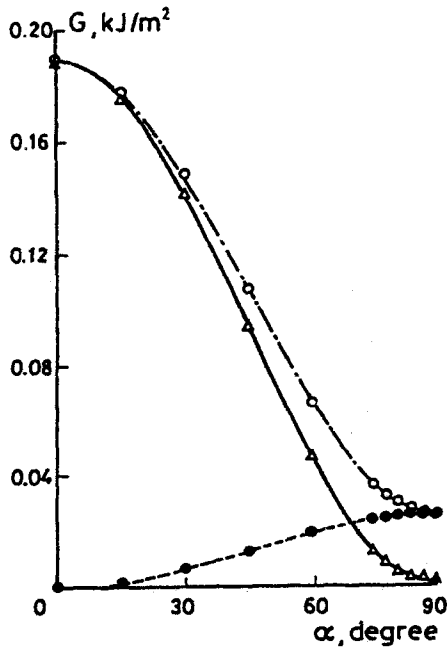


Fig. 8

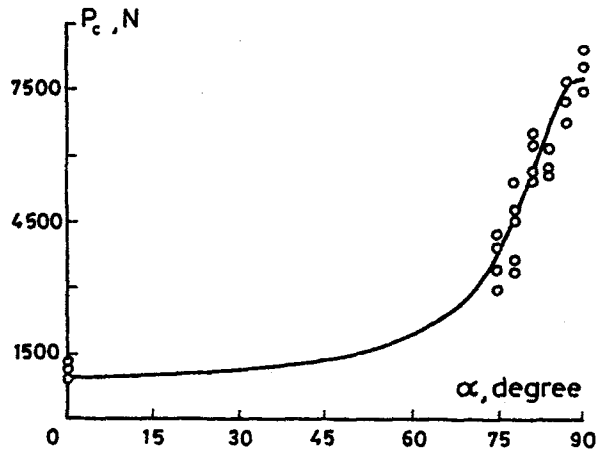


Fig. 9

Fig. 8. The G_I (Δ), G_{II} (\bullet), and $G_T = G_I + G_{II}$ (\circ) rates of the energy release versus the loading angle α of the CTS specimen for the load $P = 1000$ N.

Fig. 9. The critical load P_c versus the loading angle α of the CTS specimen. The calculation results are shown by lines and the experimental data by dots.

(8), the rate of energy release of mode I is dominant. However, for loading angles from $\alpha = 80^\circ$ to $\alpha = 90^\circ$ (see Table 1) the loading conditions of mode II at the crack tip are dominant.

The criterion (5) with $m = 1$ and $n = 2$ or the expression (8) can be written through the critical load of the structure. In the case of linear response for all parts of the structure, the relations between the rates of the energy release and the load P can be given by

$$G_I = g_1 P^2, \quad G_{II} = g_2 P^2. \quad (10)$$

Here, the parameters g_1 and g_2 depend on the geometry and properties of the material of the structure. These parameters can be obtained by the finite element solution. In the case of the CTS test, the parameters g_1 and g_2 also depend on the loading angle α . For different loading angles (see Table 1 and Fig. 5), these parameters were obtained by the finite element solution. By substituting the expressions (10) into the criterion (5) with the exponents $m = 1$ and $n = 2$, the critical loads P_c of the structure can be calculated from the equation

$$\left[\frac{g_2}{G_{IIC}} \right]^2 P_c^4 + \frac{g_1}{G_{IC}} P_c^2 - 1 = 0. \quad (11)$$

By substituting into this equation the values $G_{IC} = 0.175$ kJ/m² and $G_{IIC} = 1.561$ kJ/m² of the interlaminar fracture toughness (see Table 3) of the glass/epoxy composite, the critical loads of the CTS specimen under different loading angles can be calculated. The predicted values obtained from Eq. (11) were compared with the experimental results in Fig. 9 and good agreement was found. It should be noted that the

failure criterion can be presented through the rates of the energy release (5), the comparative energy (8), or the critical loads (11), while for the analysis of the propagation of the interlaminar crack of mixed mode in laminated composite structures the failure criterion in the form of Eq. (8) is the most convenient.

5. Conclusions

In this study, it is proposed to use a compound version of the CTS specimen for the investigation of the critical rates of the energy release of mixed mode I/II of laminated polymeric composites. A broad range of mixed mode ratios were obtained by changing the loading angle of the specimen. The highest ratio of the mixed mode obtained in the present experiments was $G_{II}/G_I = 60$. The characteristics of interlaminar fracture of the glass/epoxy composite were investigated. It has been shown that in the case of the loading conditions of pure mode I or II there are no statistically significant differences between the results obtained by the beam (DCB and ENF) and CTS tests. The energy required to drive the crack under the loading conditions of pure mode II was found to be about nine times higher than that required for pure mode I, and the energies required under the loading conditions of mixed mode I/II are between those for the pure mode. The results of the experiments of the mixed mode are used in order to obtain the parameters for the failure criterion. It has been shown that a better approximation can be achieved with linear and quadratic terms in the criterion, where the rate of the energy release of mode I is dominant.

Acknowledgments. This study was performed in the framework of the project of designing interfaces of glass fiber-reinforced composites. The project was performed in cooperation among the universities of Riga, Kassel, and Paderborn. The authors gratefully acknowledge financial support by the VW Foundation (Hannover, Germany) through Grant I/70 665. The work was partly supported also through Grant No. 96.0504 of the Latvian Council of Science.

REFERENCES

1. R. Rikards, F.-G. Buchholz, A. K. Bledzki, G. Wacker, and A. Korjakin, "Mode I, mode II, and mixed mode I/II interlaminar fracture toughness of GFRP influenced by fiber surface treatment," *Mech. Compos. Mater.*, **32**, No. 5, 439-462 (1996).
2. H. Albertsen, J. Ivens, P. Peters, M. Wevers, and I. Verpoest, "Interlaminar fracture toughness of CFRP influenced by fibre surface treatment. Part 1. Experimental results," *Compos. Sci. Technol.*, **54**, 133-145 (1995).
3. R. Rikards, F.-G. Buchholz, A. K. Bledzki, H. Wang, G. Wacker, and A. Korjakin, "Interlaminar fracture toughness of GFRP influenced by fiber surface treatment," *J. Compos. Mater.* (1998) (in press).
4. B. D. Davidson, R. Krüger, and M. König, "Three-dimensional analysis of center-delaminated unidirectional and multidirectional single-leg bending specimens," *Compos. Sci. Technol.*, **54**, 385-394 (1995).
5. S. Hashemi, A. J. Kinloch, and G. Williams, "Mechanics and mechanisms of delamination in a poly(ether sulphone) — fibre composite," *Compos. Sci. Technol.*, **37**, 426-429 (1990).
6. T. K. O'Brien, "Mixed-mode strain energy release rate effects on the edge delamination of composites," *ASTM STP 836*, 125-142 (1984).
7. M. L. Benzeggagh, P. Davies, X. J. Gong, J. M. Roelandt, M. Mourin, and Y. L. Prel, "A mixed mode specimen for interlaminar fracture testing," *Compos. Sci. Technol.*, **34**, 129-143 (1989).
8. J. R. Reeder and J. H. Crews, Jr., "Mixed-mode bending method for delamination testing," *AIAA J.*, **28**, 1270-1276 (1990).
9. A. J. Kinloch, Y. Wang, J. G. Williams, and P. Yayla, "The mixed mode delamination of fibre composite materials," *Compos. Sci. Technol.*, **47**, 225-237 (1993).
10. S. Zhao, M. Gädke, and R. Prinz, "Mixed-mode delamination behavior of carbon/epoxy composites," *J. Reinf. Plast. Compos.*, **14**, 804-826 (1995).

11. C. Hwu, C. J. Kao, and L. E. Chang, "Delamination fracture criteria for composite laminates," *J. Compos. Mater.*, **29**, 1962-1987 (1995).
12. M. Arcan, Z. Hashin, and A. Voloshin, "A method to produce plane-stress states with application to fiber-reinforced materials," *Exper. Mech.*, **18**, 141-146 (1978).
13. L. Banks-Sills, M. Arcan, and H. D. Bui, "Toward a pure shear specimen for K_{IIC} determination," *Int. J. Fract.*, **22**, R9-R14 (1983).
14. R. A. Jurf and R. B. Pipes, "Interlaminar fracture of composite materials," *J. Compos. Mater.*, **16**, 386-394 (1982).
15. S. H. Yoon and C. S. Hong, "Interlaminar fracture toughness of graphite/epoxy under mixed mode deformations," *Exper. Mech.*, **30**, 234-239 (1990).
16. A. Bansal and M. Kumosa, "Application of biaxial Iosipescu method to mixed-mode fracture of unidirectional composites," *Int. J. Fract.*, **71**, 131-150 (1995).
17. H. A. Richard and K. A. Benitz, "A loading device for the creation of mixed mode in fracture mechanics," *Int. J. Fract.*, **22**, R55-R58 (1983).
18. H. A. Richard, "Crack problems under complex loading," in: G. C. Sih, H. Nisitani, and T. Ishihara (eds.), *Role of Fracture Mechanics in Modern Technology. Proc. Int. Conference on the Role of Fracture Mechanics in Modern Technology*, Fukuoka, Japan, 2-6 June, 1986, North-Holland, Amsterdam (1987), pp. 577-588.
19. Karlson Hibbitt, *ABAQUS User's Manual, Version 5.3*, Providence Rhode Island, Sorensen Inc. (1993).
20. E. F. Rybicki and M. F. Kanninen, "A finite element calculation of stress intensity factors by modified crack closure integral," *Eng. Fract. Mech.*, **9**, 931-938 (1977).
21. E. M. Wu, "Application of fracture mechanics to anisotropic plates," *J. Appl. Mech.*, **34**, 967-974 (1967).
22. J. M. McKinney, "Mixed-mode fracture of unidirectional graphite/epoxy composites," *J. Compos. Mater.*, **6**, 164-166 (1972).
23. G. C. Sih, "Strain-energy-density factor applied to mixed mode crack problems," *Int. J. Fract.*, **10**, 305-321 (1974).
24. G. Di Leonardo, "Fracture toughness characterization of materials under multiaxial loading," *Int. J. Fract.*, **15**, 537-552 (1979).
25. J. M. Whitney, "Experimental characterization of delamination fracture," in: N. J. Pagano (ed.), *Interlaminar Response of Composite Materials*, Elsevier, Amsterdam (1989), pp. 161-250.
26. M. Charalambides, A. J. Kinloch, Y. Wang, and J. G. Williams, "On the analysis of mixed-mode failure," *Int. J. Fract.*, **54**, 269-291 (1992).
27. H. A. Richard, "Safety estimation for construction units with cracks under complex loading," in: H. P. Rossmanith (ed.), *Structural Failure, Product Liability and Technical Insurance: Proc. 2nd Int. Conference*, July 1-3, 1986, Vienna, Austria, Interscience Enterprises Ltd., Geneva (1987), pp. 423-437.